Annual Journal of Hydraulic Engineering,
JSCE VOL. 41 (1997)

Effect of Landcover Parameters on Catchment Hydrologic Process Simulation

By Dushmanta DUTTA* and Srikantha HERATH**

ABSTRACT

Distributed hydrologic models can be used to simulate hydrologic processes in a catchment considering the spatial variability of catchment characteristics such as landcover, topography and other physical parameters. Remote sensing images provide a very effective means of estimating landcover parameters of a catchment as they can be used to estimate the temporal and spatial variation of a large area at high resolution. In this study different sets of landcover maps of the Agno river basin in the Philippines were derived from satellite images using different landcover classification strategies, which include supervised, unsupervised and hierarchical classifications. The best classification images were judged by aerial photographs and site visits. Hydrological simulations were carried out with a distributed hydrologic model using different landcover maps obtained to identify the model sensitivity to the landcover data and to estimate the changes in hydrologic processes with changes in landcover patterns. Results show different components of the hydrological cycle are affected to different degree depending on landcover information.

Keywords: landcover classification, hydrologic modeling, the Agno river basin

1. INTRODUCTION

Hydrologic models are used to estimate the catchment response to the rainfall input. In recent years, with increasing computational power at hand, it is becoming possible to use physically based catchment models to describe the hydrologic processes in the catchment. These models employ the governing equations of the water flow in its various phases, and simulate its movement through rainfall, evaporation, infiltration, subsurface flow, groundwater flow and river flow. Since there are no analytical solutions to any of the governing equations, coupled numerical models are used for the solution, which make it necessary to discretize the catchment into a number of grids, in the horizontal and vertical planes. Also due to the nature of the governing equations, it is necessary to assume these units to be homogeneous in relation to some hydrologic properties, such as soil hydraulic characteristics. Therefore in order to set up a distributed hydrologic model, a large amount of both spatial and temporal input data should be prepared. The major required spatial datasets are topography, river network, landcover pattern, soil types and groundwater aquifer and aquitard layers. Time series data are rainfall, river discharge and water levels, evaporation, leaf area index (LAI), root distribution function (RDF), and groundwater withdrawal. Once such models are prepared they can be used to estimate spatial distribution of different hydrologic variables such as overland and stream flows, evapotranspiration, groundwater heads and soil moisture distribution. One important area of application of distributed models is the assessment of landcover change on the hydrologic regime.

Remote sensing data are an important source to estimate landcover parameters effectively over a large area at high resolution. They are attractive as means of obtaining temporal variation of landcover and to study its effect on hydrologic parameters. Therefore, it is important to identify the limitations of using satellite data in terms of sensitivity to the classification methods especially, if such techniques are to be used in forecasting effects of landcover changes to the hydrologic environment. In this paper, we have used different sets of landcover maps derived from same satellite image for hydrologic simulation to assess the effect of landcover parameters in hydrologic processes.

2. STUDY AREA

A sub catchment of the Agno river basin, the fifth largest river basin in the Philippines which lies in the western portion of the central part of Luzon island from 120°00' to 121°00' east longitude and 15°00' to 16°45' north latitude with a drainage area of 5,952 km^2, is selected as the study area (*National Water Resources Council,*

* Member, Research Associate, IIS, University of Tokyo (7-22-1 Roppongi, Minato-ku, Tokyo 106)
** Member, Guest Professor, IIS, University of Tokyo (7-22-1 Roppongi, Minato-ku, Tokyo 106)

1983)[1]. The sub catchment encompasses an area of 1,700 km^2 and it is an ideal site for this study as both satellite images and data required for hydrological model simulation are available for this part of the basin(*Fig. 1*). The annual average rainfall varies from 2,000 mm in the south-eastern part of the study area to more than 4,000 mm in the northern mountainous area.

The study area can be distinctly divided into two parts based on the variation of landcover pattern i.e. the upper mountainous area and lower flat area. The vegetation of the upper mountainous area includes dense and light forest areas, whereas lower flat area is covered by agricultural fields and grass lands. In the lower part, along the Agno river, residential areas are visible.

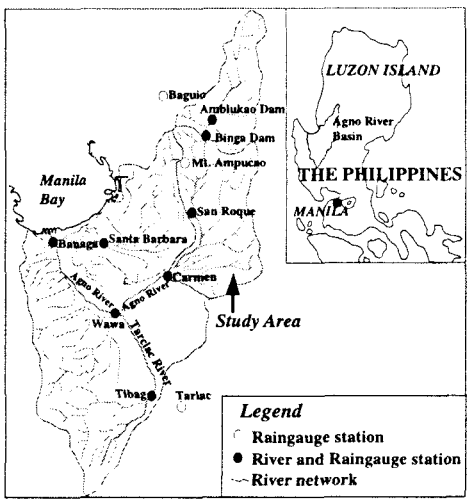

Fig. 1 Agno river basin, the Philippines

3. MODEL BACKGROUND

Presently several distributed models are being applied to real-world problems. Among them are the Systeme Hydrologique Europeen (SHE) model (*Abbott et al., 1986*)[2], probably the best known model of its kind at present, KINEROS model (*Smith, 1977*)[3], ANSWERS model (*Beasley and Huggings, 1982*)[4], IHDM model (*Beven et al., 1987*)[5] etc. In this study, SHE model has been used for hydrologic analyses. In this model, kinematic approximation of St. Venant equations is used to simulate the overland and stream flows. The Kristensen and Jensen model (*Kristensen and Jensen, 1975*)[6] is used for calculation of evapotranspiration. The unsaturated zone flow is simulated by 1-D Richards' equation and 3-D non-linear Boussinesq equation is solved numerically for ground water simulation. In the SHE model, finite difference solution schemes are used to solve the governing equations using square and regular grid system.

Landcover patterns play a vital role in governing the hydrologic processes in a catchment. Mainly, the surface runoff, interception and evapotranspiration components vary to a large extent depending upon the type of landcover and thus, the subsurface storage varies. In a physically based distributed model, mainly three input parameters vary with the variation of landcover patterns. They are: 1. Surface roughness coefficients, 2. Time series data of LAI, and 3. Time series data of RDF. The evaporation from soil and transpiration from vegetation depends on the density of the crop extent, described by LAI, and the actual soil moisture content in the nodes in the root zone. Transpiration also depends on the root density. In SHE model, the governing equations used for evapotranspiration and interception are as follows:

Transpiration: $E_{at} = f_1(LAI)*f_2(\theta)*RDF*E_p$

where,

$f_1(LAI) = C_1*LAI + C_2$ *for* $f_1(LAI) < 1$

$= 1$ *for* $f_1(LAI) > 1$

$f_2(\theta) = 1 - [(\theta_F - \theta)/(\theta_F - \theta_w)]^{(C3/Ep)}$

E_p = *potential evapotranspiration*

θ_F = *volumetric moisture content at field capacity*

θ_w = *volumetric moisture content at wilting point*

θ = *volumetric moisture content*

C_1, C_2 *and* C_3 *are empirical parameters (mm/day)*

Evaporation: $E_s = E_p*f_3(\theta)+(E_p-E_{at}-E_p*f_3(\theta))*f_4(\theta)$

where,

$f_3(\theta) = C_2*(\theta/\theta_w)$ *for* $\theta_M \le \theta \le \theta_w$

$= C_2$ *for* $\theta \ge \theta_w$

$= 0$ *for* $\theta \le \theta_M$

$f_4(\theta) = [\{\theta - 0.5*(\theta + \theta)\}/\{\theta - 0.5*(\theta_w + \theta_F)\}]$ *for* $\theta > 0.5*(\theta_w + \theta_F)$

$= 0$ *else*

Interception storage capacity: $I_{max} = C_{int}*LAI$

where,

C_{int} = *interception parameter*

4. SINGLE COLUMN ANALYSIS

4.1 Methodology

To understand effect of landcover patterns on hydrologic processes, a single column analysis has been performed with six different types of landcover classes. The six landcover classes considered the analysis were selected based on the actual landcover types of the study, as follows:

1. Agriculture land, 2. Bare land, 3. Built-up area (impervious ratio: 40%), 4. Forest, 5. Grass land and 6. Bush land. The time series data for LAI (*Fig. 2*) and RDF for different landcover types have been collected from various available sources (*Diskinson et al., 1993*) [7]. Simulation for one year period for the six landcover parameters were carried out using SHE model. The other input parameters and hydrological time series data were kept same for all the six cases.

4.2 Results from Single Column Analysis

Figure 3 shows the water balance of different hydrological components such as total evapotranspiration, unsaturated zone storage and groundwater storage obtained from the model simulations after one year period. In case of forest land, evapotranspiration becomes much higher than the other components whereas, groundwater storage becomes the highest in bare land. Thus, a distinct variation in distribution of water in hydrologic processes for different landcover classes can be realized.

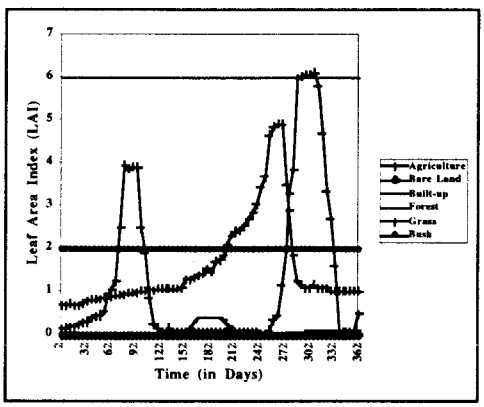

Fig. 2 Time series of LAI for different landcover classes

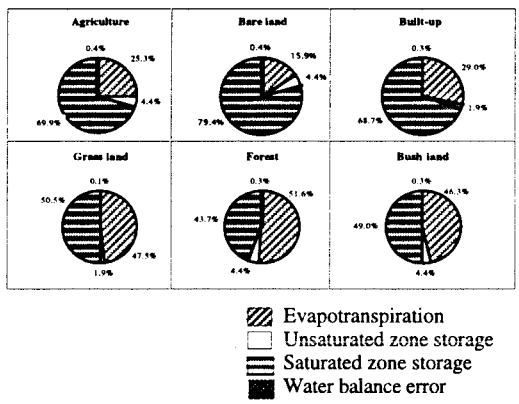

Fig. 3 Water balance for different landcover classes (from single column analysis)

5. DERIVATION OF LANDCOVER PATTERNS

5.1 Image Selection & Geometric Correction

The SPOT HRV digital images are used for this study for landcover classification. The digital data was acquired for the study area for January 10, 1993, processed at the 1B level by SPOT Image Corp. After importing the dataset to the proper digital format, it was overlayed with the catchment boundary and river network data, digitized from 1:50,000 scale maps, to verify the geometric correctness of the dataset. Transformation and rectification of the image were done using the digitized river network for geometric correction of the dataset.

5.2 Supervised Classification

Supervised classification using the original bands and their subsequent transformations into NDVI (Normalized Difference Vegetation Index) [*NDVI = (Infrared - Red)/(Infrared + Red)*] and Soil Brightness Index [*SBI = (0.332 x Green) + (0.603 x Red) + (0.262 x Infrared)*] were performed to determine accuracy of identification of different landcover classes utilizing the satellite data. The maximum likelihood and minimum distance classification algorithms were used in the classification.

Training areas for supervised classification were taken from the aerial photographs available for the lower part of the study area, whereas for upper part of the basin, photographs taken during field visits were used to define the training areas. Training areas were selected uniformly for these classes. Supervised classification was performed using the selected training areas initially, for original three bands. The outcome was not satisfactory compared to the available ground truth data, and hence, further supervised classifications were conducted by changing the ratios of training areas and using additional bands i.e. NDVI and SBI. The resulting landcover classes were compared with the aerial photographs. However, the outcomes from further supervised classifications were also not satisfactory for some classes to the expected degree of accuracy. Hence, a more comprehensive approach was taken to classify the image using hierarchical statistical processing procedure (*Baumgartner and Apel, 1996*)[8].

5.3 Hierarchical Statistical Processing Procedures

These procedures represent a more refined approach for classifying remote sensing data. Instead of processing all spectral bands with a large number of categories in one step, the number of spectral bands and categories is adapted to a specific problem. Density slicing of each band was carried out to identify the range of reflectance values representing different classes and non-representative parameters were classified further using either supervised or unsupervised learning techniques after extracting the representative parameters. Depending on the

problem, several classifications - each resulting in a bit mask (thematic maps) - are carried out. After this multi-step classification, all the resulting bit masks are combined into final classification map.

5.4 Image Classification: Results and Discussion

Based on the field data and prior knowledge of major distinct landcover patterns in the study area, a total of eight landcover classes were categorically selected as landcover types. They are: 1) Agriculture, 2) Grass land, 3) Bush and small branches of tree, 4) Forest, 5) Bare/rocky land, 6) Built-up area, 7) Water body, and 8) Reservoir.

The results obtained from three supervised classifications with different ratios of training areas and with additional bands (*Table 1*) show high variation of landcover classes agriculture, bared/rocky land and built-up area with the changes of total training areas and with the incorporation of additional bands. By comparing these classified landcover classes with ground truth data such as aerial photographs and field photographs, it can be clearly seen that a few classes such as reservoir, water body and forest are representative of actual field conditions, while a clear distinction between the other classes is not possible. Also, no definite trend could be found from the changing of area percentage of training area leading to a robust procedure to classify the images.

In the hierarchical statistical processing procedures (*Fig. 4 and Table 1*), after, density slicing of the three bands, unsupervised classification was done using band 1, band 2 (> 17), band 3 (< 70), NDVI (< 70%) and SBI band for remaining five classes. From the classified image, only bare/rocky land class was visible as representative of actual class. Supervised classification was done for remaining classes using training areas based on ground truth information. The process was done many times modifying the training area ratios to obtain representative output. The final classified image shows that the three classes (agriculture, bush and grass) are well representative of real situation. However, built-up area takes some cells which represent agriculture areas in reality. It may be due to similar reflectance of these areas as the image was taken in the month of January, which is not the cultivation season in the basin. The resulting thematic maps obtained in the whole process are combined into the final classification map (*Figs. 5 & 6*).

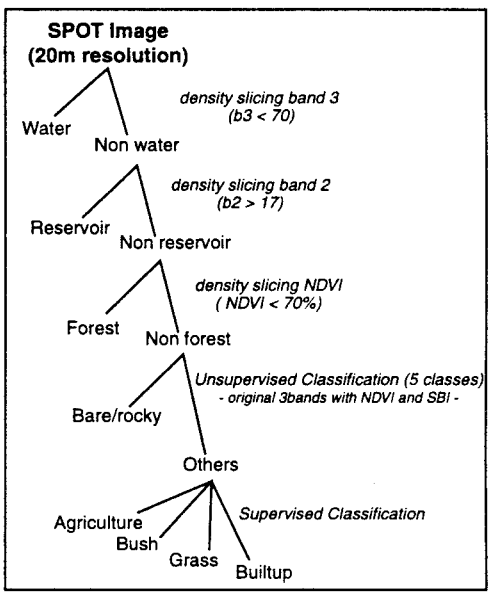

Fig. 4 Dendrogram for a multi-step hierarchical classification of SPOT image

Table 1 Area statistics of landcover classes obtained from different classification schemes

Landuse Classes	*Supervised classification*						*Case IV Hierarchical classification*
	Case I Original three bands		*Case II 3 bands with changed training areas*		*Case III Original three bands with NDVI and SBI bands*		
	Area of each class (Km^2)	Training area (Km^2)	Area of each class (Km^2)	Training area (Km^2)	Area of each class (Km^2)	Training area (Km^2)	Area of each class (Km^2)
Bare/Rocky land	*268.53* (6.7%)	0.05 (0.6%)	*110.16* (2.8%)	0.01 (0.1%)	*309.13* (7.8%)	0.02 (0.1%)	*637.17* (16.0%)
Forest	*712.91* (17.9%)	0.03 (0.3%)	*738.78* (18.5%)	2.82 (27.3%)	*753.07* (18.9%)	2. 92 (27.3%)	*154.60* (3.9%)
Agriculture	*759.43* (19.0%)	3.93 (46.3%)	*1009.77* (25.3%)	3.58 (34.6%)	*639.01* (16.0%)	3.66 (34.2%)	*728.65* (18.3%)
Reservoir	*7.15* (0.2%)	0.55 (6.5%)	*7.05* (0.2%)	0.51 (4.9%)	*7.38* (0.2%)	0.52 (4.8%)	*3.08* (0.1%)
Bush land	*775.26* (19.4%)	0.87 (10.3%)	*936.82* (23.5%)	0.77 (7.5%)	*896.37* (22.5%)	0.79 (7.4%)	*1115.62* (28.0%)
Water body	*29.69* (0.7%)	0.61 (7.2%)	*33.49* (0.8%)	0.61 (5.9%)	*32.51* (0.8%)	0.67 (6.2%)	*71.45* (1.8%)
Grass land	*813.95* (20.4%)	2.24 (26.5%)	*909.54* (22.8%)	2.04 (19.7%)	*842.04* (21.1%)	2.08 (19.4%)	*1037.83* (26.0%)
Built-up area	*619.99* (15.6%)	0.19 (2.2%)	*241.32* (6.1%)	0.01 (0.1%)	*507.39* (12.7%)	0.05 (0.5%)	*238.52* (5.9%)
Total	*3986.92* (100.0%)	8.47 (100.0%)	*3986.92* (100.0%)	10.35 (100.0%)	*3986.92* (100.0%)	10.69 (100.0%)	*3986.92* (100.0%)

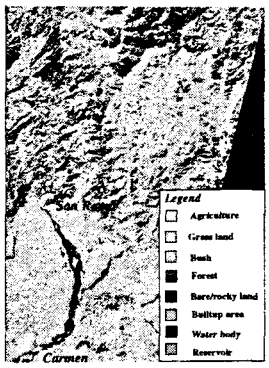

Fig. 5 Classified image from hierarchical statistical processing procedures

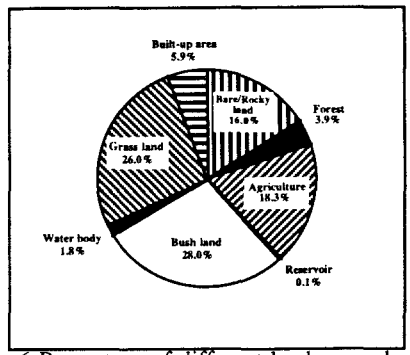

Fig. 6 Percentage of different landcover classes

6. HYDROLOGIC MODELING

6.1 Methodology

Required spatial and temporal data were collected from possible agencies in the Philippines and a GIS was developed for spatial data to handle the extensive amount of data precisely (*Dutta and Herath, 1996*)[9]. The drainage network was generated from the 50 m resolution digital elevation model (DEM) which was developed from digitized contours of 1:50,000 scale topography maps (*Fig. 7*).

The two landcover classes obtained from supervised and hierarchical classifications (Cases I & IV of Table 1) have been used in the model as input data for two simulations. Considering the availability of temporal data, time period for the model simulation is chosen as July 1 to August 20, 1989 which falls in rainy season and experienced a severe typhoon. Within the period of 1985 to 1993, only three sets of SPOT images could be obtained for the study area, they were of years 1987, 1988 and 1993. However, except the images of 1993, no other image was cloud free. Hence, it was decided to use the image of year 1993, which is considered to be adequate enough to represent the landcover for 1989 as the changes of landcover pattern in the study area within the period were not very significant.

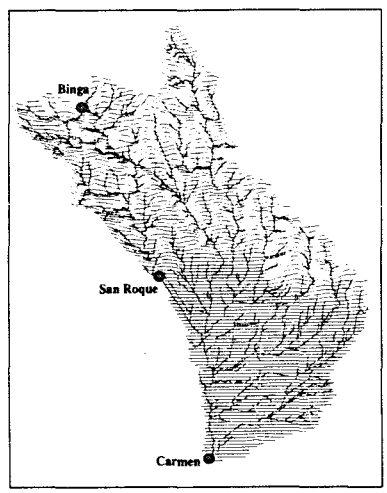

Fig. 7 DEM of the study area (500m resolution) and generated river

6.2 Hydrologic modeling: Results and Discussion

In the two different scenarios of model simulation, input data were kept same except for landcover classes and its associated data such as surface roughness coefficients, time series of LAI and RDF for different landcover patterns. Table 2 shows the water balance for the simulation duration with the value for each component of hydrologic cycle for the two cases.

The results of the two cases show significant variation in model outputs with different input landcover information. Figure 8 shows the temporal variation of different hydrologic components for the two cases of simulation. From the Table 2 it can be seen that both evapotranspiration and the surface runoff are significantly affected whereas moisture storage is affected to a lesser degree. This can be attributed to the direct dependency of evapotranspiration on leaf area index, which is related to landcover, and the dependency of overland flow on surface roughness which depends also on the landcover. On the other hand, as we did not alter the soil hydraulic property distribution, moisture storage is slightly affected. It should be noted that the differences are significant considering the short time period simulated, less than two months.

Table 2 Total water balance components for the simulation results (period July 1- August 20, 1989)

No.	*Total Rainfall*	*Total Evapotranspiration*	*Water stored in surface*	*Water stored in river*	*Accumulated net river flow*	*Unsaturated Zone storage*	*Water balance error*
Case I	830	141	35	9	9	642	6
Case IV	830	127	26	11	17	657	8
Relative Changes (case I - case II)/case I		9.9%	25.7%	18.2%	88.9%	2.3%	33.3%
Absolute Changes (case I - case II)/Rainfall		1.7%	1.1%	0.2%	1.0%	1.8%	0.2%

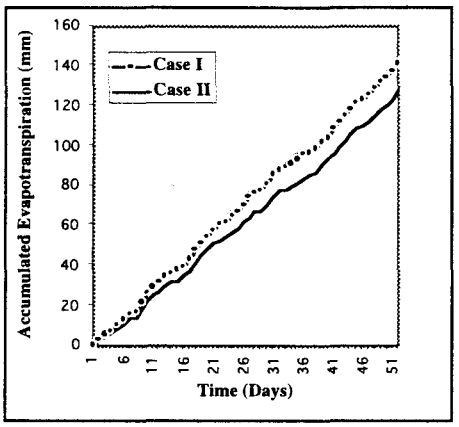

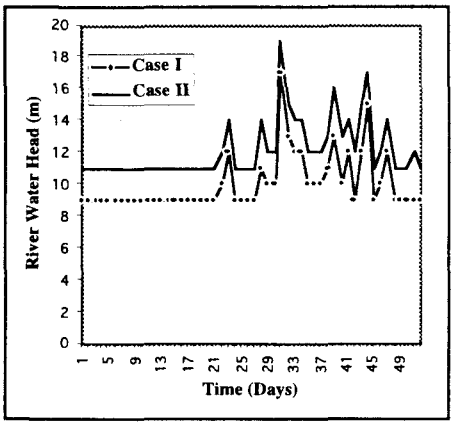

Fig. 8 Simulated temporal distribution of hydrologic components of the two cases

7. CONCLUSION

Physically based hydrologic models are formulated based on the governing equations of different hydrologic components and can be expected to provide realistic hydrologic simulation based on basin characteristics. It is necessary to have precise input data to setup such models for simulation. From the results of this study, impact of landcover information on simulation results is seen to be significant. This implies that when distributed hydrologic models are used to assess the environmental impact of landcover changes, the setting up of landcover information should be carried out carefully. As only remote sensing data provide a viable method to obtain these information, further research is needed for improved image classification algorithms.

REFERENCES

1) National Water Resources Council (1983): Agno River Basins, National Water Resources Council, Republic of the Philippines, Report no. 24-3B.

2) Abbott, M.B., Bathers, J.C., Cunge, J.A., O'Connell, P.E. & Rasmussen, J. (1986): An Introduction to the European Hydrologic System - Systeme Hydrologique Europeen, 'SHE', 1: History and Philosophy of a physically-based Distributed Modelling System, Journal of Hydrology, Vol. 87, pp. 45-59.

3) Smith, R.E. (1977): Field test of a distributed watershed erosion/sedimentation model. In: Soil Erosion: Prediction and Control, Proceedings of National Conference on Soil Erosion, SCSA Special Publication, No. 21, Ankeyny, IA, pp. 201-209.

4) Beasley, D.B. and Huggins, L.F. (1982): ANSWERS Users Manual, EPA-905/9-82-001, United States Environmental Protection Agency (USEPA), Region V, Chicago, IL.

5) Beven, K.J., Calver, A. and Morris, E. M. (1987): The Institute of Hydrology Distributed Model, Institute of Hydrology, Report No. 98, Wallingford.

6) Kristensen, K.J. and Jensen, S.E. (1975): A Model for Estimating Actual Evapotranspiration from Potential Evapotranspiration, Nordic Hydrology, Vol. 6, pp. 70-88.

7) Diskinson, R.E., Henderson-Sellers, A., Kennedy, P. J. (1993): Biosphere Atmosphere Transfer Schemes (BATS) version 1e, as coupled to the Community Climate Model, NCAR Technical Note NCAR/TN-387+STR, National Center for Atmospheric Research, Boulder, Co.

8) Baumgartner, M.F. and Apel, G.M. (1996): Remote sensing and geographic information systems, Hydrological Sciences Journal, 41(4) August 1996, pp.593-607.

9) Dutta, D. and Herath, S. (1996): Development of a GIS for the hydrologic analysis of Agno river basin, the Philippines, Proceedings of Japan Society for Civil Engineering (JSCE) conference, 1996, pp. 334-335.